

# Low-Melting-Point Titanium-Base Brazing Alloys— Part 1: Characteristics of Two-, Three-, and Four-Component Filler Metals

*E. Chang and C.-H. Chen*

The melting point, microstructure, phase, and electrochemical behavior of Ti-21Ni-15Cu alloy, together with two-, three-, and four-component low-melting-point titanium-base brazing alloys, are presented in this paper. Five filler metals were selected for the study, in which melting points were measured by differential thermal analysis, phases identified by x-ray diffractometry, and corrosion behaviors tested by potentiodynamic polarization. The experimental results show that the three-component Ti-15Cu-15Ni and the newly developed Ti-21Ni-14Cu alloys exhibit the combination of lower melting point and superior corrosion resistance compared to the two- and four-component titanium alloys, 316L stainless steel, and a Co-Cr-Mo alloy in Hank's solution at 37 °C. On a short time basis, the presence of Ti<sub>2</sub>Ni and Ti<sub>2</sub>Cu intermetallics in the Ti-15Cu-15Ni and Ti-21Ni-14Cu alloys should not be preferentially dissolved in galvanic corrosion with respect to the dissimilar Ti-6Al-4V alloy.

**Keywords** braze alloys, electrochemical property, filler metal, melting point, phase, Ti-Ni-Cu alloys, titanium

## 1. Introduction

Although titanium alloys may be joined by fusion welding, resistance welding, diffusion bonding, brazing, and so forth, brazing offers the advantage of being able to join easily rather complicated and precise components (Ref 1, 2). In industry, silver-base filler such as Ag-Cu-Ni-Li (Ref 3), aluminum alloys (Ref 4), and titanium-base alloys (Ref 5, 6) are widely used as filler metals for titanium alloy brazing. Among them, titanium-base alloys possess excellent mechanical properties and good corrosion resistance (Ref 5, 6). Through the development of titanium-base fillers, the pursuit of lower-melting-point alloys to below the  $\beta$  transus or even lower temperature has interested metallurgists (Ref 5, 7). Brazing at lower temperature for titanium alloys not only minimizes the lamellar structure at the weld reaction zone, but also retards grain growth. Lamellar structure and coarse grain size are known to deteriorate the high-cycle fatigue strength of welded titanium alloys (Ref 8, 9). Under the same condition of brazing, a lower-melting-point filler metal may also provide the indispensable fluidity and wettability that guarantee that the filler metal can satisfactorily fill the cavity assisted by capillary force and be in good contact with the base metals (Ref 10).

Recently, a low-melting-point titanium filler metal of the chemical composition Ti-21Ni-14Cu was explored, and the brazing conditions of the alloy reported (Ref 11). A reasonably good corrosion resistance of the alloy is of interest for its application. This work aims at assessing the potentiality of the newly developed Ti-21Ni-14Cu titanium filler metal for brazing in terms of the important characteristics of melting temperature and corrosion resistance. This paper reports the preliminary result of microstructure, phase, melting point, and

potentiodynamic data of Ti-21Ni-14Cu alloy in comparison with other two-, three-, and four-component titanium alloys and several commercial alloys.

## 2. Materials and Methods

Five titanium-base filler metals of the compositions Ti-28Ni, Ti-15Cu-15Ni, Ti-21Ni-14Cu, Ti-35Zr-15Cu-15Ni, and Ti-42.5Zr-10Cu-5Ni were chosen for study of corrosion resistance. The reason for the choices was based on their potentiality for low melting temperature. The filler metals of each composition were prepared using titanium, copper, nickel, and zirconium metal powders of more than 99.7% purity with -325 mesh. After mixing, each material was melted and solidified in a graphite crucible under a vacuum of  $\sim 1.4 \times 10^{-4}$  Pa. For microstructural observation, the solidified ingots were ground, polished, and swab etched with Kroll's solution (3 mL Hf, 36 mL HNO<sub>3</sub>, 100 mL H<sub>2</sub>O) for 15 s and then examined in a Nikon optical microscope (Nikon Corporation, Tokyo, Japan). X-ray diffractometer (XRD) (Rigaku D/Max III, V; Rigaku Corporation, Tokyo, Japan) was operated at the voltage of 30 KV, cur-

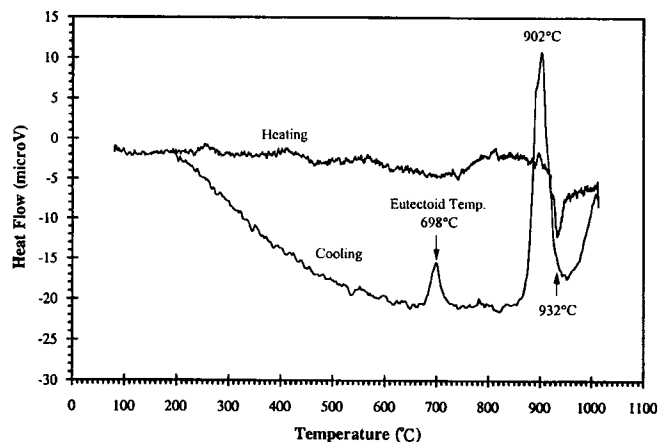


Fig. 1 DTA analysis of Ti-21Ni-14Cu alloy

**E. Chang and C.-H. Chen**, Department of Materials Science and Engineering, National Cheng-Kung University, Tainan 701, Taiwan.

rent of 20 mA and scanning speed of 4°/min for phase identity using Cu K $\alpha$  radiation. The mixed metal powders were heated at 5 °C/min to above the melting temperature and then furnace cooled for melting-point measurements using a differential thermal analyzer (DTA) (Setaram, Tag 24; Setaram Corporation, Cedex, France), and the previously solidified ingots for metallography were used for corrosion-resistance tests.

The potentiodynamic polarization assessments of the titanium filler metals, together with the controls of AISI type 316L stainless steel, Co-Cr-Mo alloy (ASTM F75), Ti-6Al-4V, and commercially pure (cp) titanium, were conducted using EG&G PAR M273 potentiostat (EG&G Instruments Corporation, Princeton, New Jersey) in deaerated Hank's solution at 37 °C per ASTM G 61 and ASTM G 5 standards. The solution contains 8.0 g NaCl, 0.14 g CaCl<sub>2</sub>, 0.4 g KCl, 0.35 g NaHCO<sub>3</sub>, 1.0

g glucose, 0.10 g MgCl<sub>2</sub>·6 H<sub>2</sub>O, 0.06 g Na<sub>2</sub>HPO<sub>4</sub>·2H<sub>2</sub>O, 0.06 g KH<sub>2</sub>PO<sub>4</sub>, and 0.06 g MgSO<sub>4</sub>·7H<sub>2</sub>O per liter distilled water. The polarization started at about 200 mV cathodic to corrosion potential ( $E_{corr}$ ) (versus saturated calomel electrode, or SCE) and scanned to anodic polarization at a speed of 0.2 mV/s. When the anodic polarization was increased beyond pit nucleation potential or breakdown potential ( $E_b$ ), or the measured current density over 1000  $\mu$ A/cm<sup>2</sup>, the scan direction was reversed until the pit protection potential ( $E_{pp}$ ) was measured. The details of the similar experimental procedures are described elsewhere (Ref 12, 13).

### 3. Results and Discussion

The basis of choosing the five different filler metals are explained as follows. Of the two-component titanium-base alloys, Ti-28Ni demonstrated the lowest melting point. In the 1970s, a commercial three-component alloy, Ti-15Cu-15Ni, with a melting point of 934 °C became available primarily for brazing aircraft components; thus the composition was selected for study. In 1990, another three-component alloy, Ti-21Ni-14Cu, was developed by Chen (Ref 11) with a reported

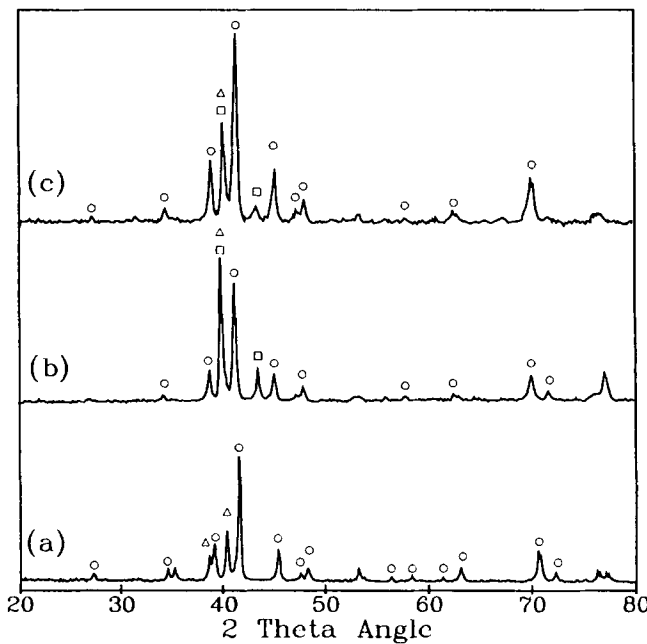


**Fig. 2** XRD result of (a) Ti-28Ni, (b) Ti-15Cu-15Ni, and (c) Ti-21Ni-14Cu alloys. open triangle,  $\alpha$ -Ti; open circle, Ti<sub>2</sub>Ni; open square, Ti<sub>2</sub>Cu

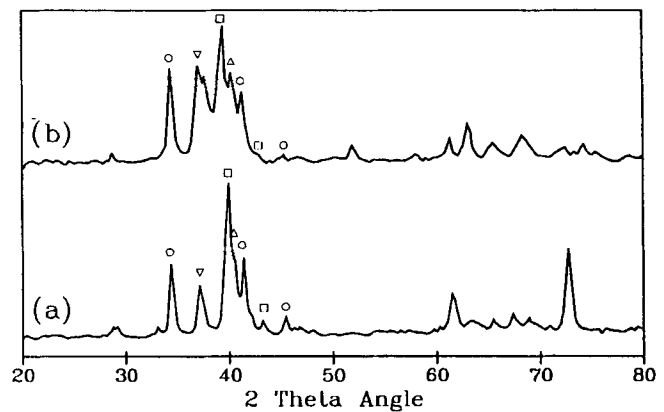


**Fig. 3** XRD result of (a) Ti-35Zr-15Cu-15Ni and (b) Ti-42.5Zr-10Cu-5Ni alloys. open triangle,  $\alpha$ -Ti; open circle, Ti<sub>2</sub>Ni; open square, Ti<sub>2</sub>Cu; open inverted triangle, Zr<sub>2</sub>Cu

**Table 1** Melting points and parameters from the potentiodynamic polarization curves of five filler metals, Co-Cr-Mo (ASTM F75), 316L stainless steel, and cp titanium in deaerated Hank's solution at 37 °C

Materials	Melting point		$E_{corr}$	$i_{corr}$	$E_{cr}$	$i_{cr}$	$i_p$	$E_b$	$E_{pp}$	$E_b - E_c$	$E_b - E_p$
	°C										
Ti-28Ni	960		-667	0.04	-333	0.87	1.65	910	734	1243	176
Ti-15Cu-15Ni	943		-751	0.07	-595	0.75	0.95	949	...	1544	...
Ti-21Ni-14Cu	916		-720	0.04	-337	0.76	1.03	926	848	1263	78
Ti-35Zr-15Cu-15Ni	820(a)		-573	0.06	-396	0.69	0.89	-149	-287	247	138
Ti-42.5Zr-10Cu-5Ni	800(a)		-934	0.05	-628	0.98	0.98	61	-88	689	149
316L stainless steel	...		-647	0.05	-496	0.38	0.89	371	-178	867	549
Co-Cr-Mo alloy	...		-623	0.03	-344	0.47	1.66	643	321	987	322
Ti-6Al-4V	...		-918	0.01	-550	0.65	0.70	2400	...	2950	...
cp titanium	...		-101	0.12	-413	0.75	0.75	>3000	...	>3400	...

Current density:  $\mu$ A/cm<sup>2</sup>, potential: mV versus SCE.  $E_{corr}$ : corrosion potential;  $i_{corr}$ : corrosion current density;  $E_{cr}$ : critical potential for active-to-passive transition;  $i_{cr}$ : critical current density for active-to-passive transition;  $i_p$ : passive current density;  $E_b$ : breakdown potential;  $E_{pp}$ : pit protection potential. (a) Adopted from Ref 7

low melting point of 917 °C; hence the composition was taken into consideration. Several four-component titanium-base filler metals with still lower melting point (~800 °C) were investigated by Onzawa et al. (Ref 7), and the two compositions of Ti-35Zr-15Cu-15Ni and Ti-42.5Zr-10Cu-5Ni were chosen for electrochemical study.

Differential thermal analysis results of the five filler metals investigated are shown in Table 1; among the materials studied, Ti-28Ni alloy possesses the highest melting point at 960 °C and Ti-42.5Zr-10Cu-5Ni alloy possesses the lowest melting point of 800 °C. Figure 1 shows the heating and cooling curves of Ti-21Ni-14Cu and shows that the melting point corresponds to the endothermic peak at 932 °C in heating cycle and exothermic peak at 902 °C in cooling cycle. The average of the two temperatures (i.e., 917 °C) was taken as the melting point of the alloy. The melting point of Ti-21Ni-14Cu alloy is lower than the commercially known two- and three-component titanium filler metals. In general, the melting points decrease with an increase of alloy content. The constituent phases in each alloy were identified by XRD, and the results are shown in Fig. 2 and 3. The Ti-28Ni alloy contains Ti<sub>2</sub>Ni (JCPDS 18-898) intermet-

allic phase, and the Ti-15Cu-15Ni and Ti-21Ni-14Cu alloys contain Ti<sub>2</sub>Ni and Ti<sub>2</sub>Cu (JCPDS 15-717) intermetallics. For Ti-35Zr-15Cu-15Ni and Ti-42.5Zr-10Cu-5Ni alloys, Ti<sub>2</sub>Ni, Ti<sub>2</sub>Cu, and Zr<sub>2</sub>Cu (JCPDS 18-466) intermetallics were identified. In all the furnace-cooled ingots, α titanium (JCPDS 44-1294) rather than β titanium phase (JCPDS 44-1288) is identified. The absence of β titanium phase in the furnace-cooled ingots is rationalized by the eutectoid decomposition of this phase in the eutectoid reaction at, for example, 698 °C for Ti-21Ni-14Cu alloy (Fig. 1). Figure 4 shows the optical micrographs of the five titanium fillers investigated; the microstructures contain α titanium phase (light) and intermetallics (dark).

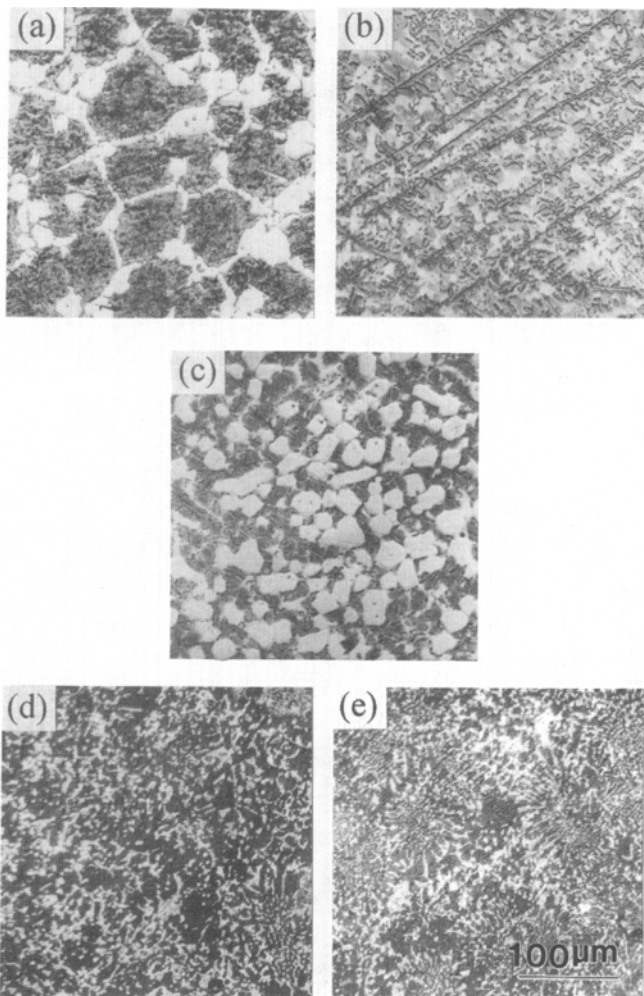


**Fig. 4** Optical micrographs of (a) Ti-28Ni, (b) Ti-15Cu-15Ni, (c) Ti-21Ni-14Cu, (d) Ti-35Zr-15Cu-15Ni, and (e) Ti-42.5Zr-10Cu-5Ni alloys

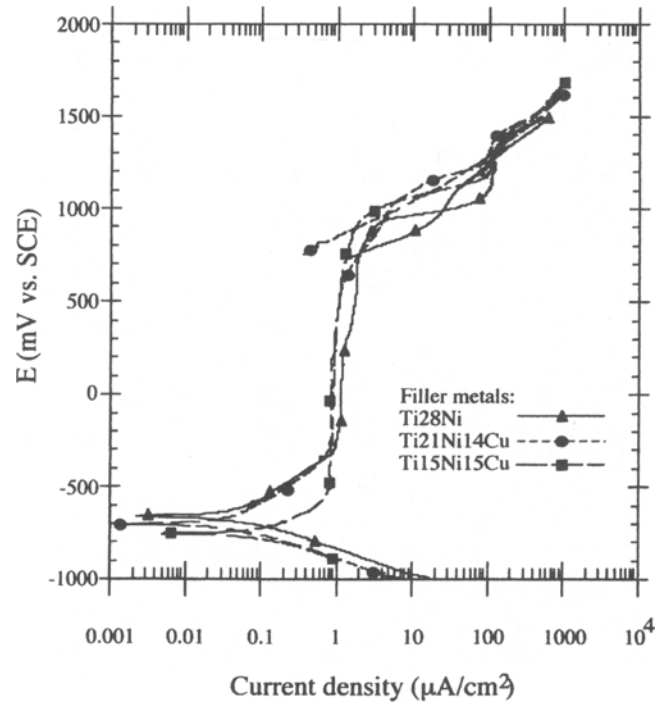


**Fig. 5** Potentiodynamic polarization curves of Ti-28Ni, Ti-15Cu-15Ni, and Ti-21Ni-14Cu alloys

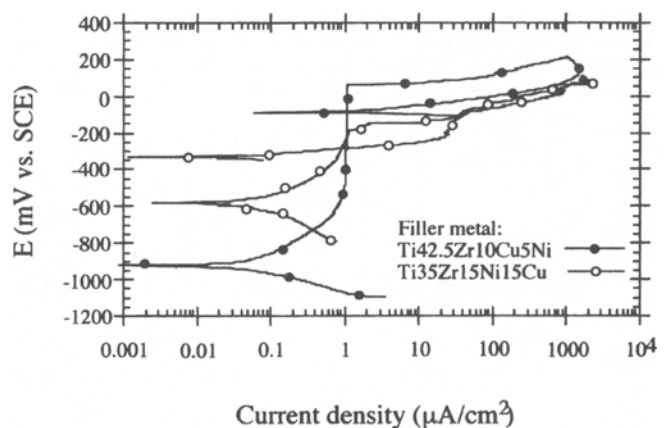


**Fig. 6** Potentiodynamic polarization curves of Ti-35Zr-15Cu-15Ni and Ti-42.5Zr-10Cu-5Ni alloys

The polarization curves of Ti-28Ni, Ti-15Cu-15Ni, and Ti-21Ni-14Cu alloys are shown in Fig. 5, and the curves of Ti-42.5Zr-10Cu-5Ni and Ti-35Zr-15Cu-15Ni alloys are shown in Fig. 6. The parameters from the potentiodynamic polarization of the five filler metals, together with 316L stainless steel, Co-Cr-Mo alloy, Ti-6Al-4V, and cp titanium, are presented in Table 1. Examination of the polarization curves for the five titanium fillers shows that all the alloys except Ti-35Zr-15Cu-15Ni alloy exhibit the distinctive passivity range (defined as  $E_b - E_{cp}$ ) without showing an active-to-passive peak. The current densities at passive zone are lower than  $2 \mu\text{A}$  in all alloys, indicating a low dissolution rate of the passive film. The two-component Ti-28Ni and three-component Ti-15Cu-15Ni and Ti-21Ni-14Cu alloys, shown in Fig. 5, possess the passivity ranges larger than 1200 mV and  $E_b$  larger than 900 mV versus SCE. The measured values of  $E_b$  for the Ti-28Ni, Ti-15Cu-15Ni, and Ti-21Ni-14Cu are distinctively higher than the equilibrium potential of oxygen generation (evolving  $\text{O}_3$  or  $\text{H}_2\text{O}_2$ ), which occurs at about 810 mV versus SCE in pH 7.4 Hank's solution at 37 °C (Ref 14).

The two-component Ti-28Ni exhibits both a low melting point (960 °C) and a large  $E_b - E_{cr}$  value (1243 mV). Significantly, the three-component Ti-15Cu-15Ni and Ti-21Ni-14Cu alloys show even lower melting points and higher  $E_b$  and  $E_b - E_{cr}$  values than the Ti-28Ni alloy, as shown in Table 1. The Ti-21Ni-14Cu alloy also shows a smaller  $E_b - E_{pp}$  value as compared with the value for Ti-28Ni alloy, indicating that the former alloy repassivates more readily. It is thus concluded that the three-component Ti-15Cu-15Ni and Ti-21Ni-14Cu alloys may have the combined characteristics of both low melting point and corrosion resistance for brazing alloy. The corrosion resistance of four-component Ti-42.5Zr-10Cu-5Ni and Ti-35Zr-15Cu-15Ni alloys are considered inferior as the passivation ranges are comparatively small and the pit protection potentials are low. Figure 7 compares the polarization profiles of Ti-21Ni-14Cu alloy along with the data of 316L stainless steel, Co-Cr-Mo alloy, Ti-6Al-4V, and cp titanium. This figure and Table 1 indicate that the 316L stainless steel and Co-Cr-Mo alloy show remarkably larger repassivation loops or larger  $E_b - E_{pp}$  values, indicating that repassivation of these materials is energetically barricaded. The breakdown potential of Ti-21Ni-14Cu alloy is much higher than the 316L stainless steel and Co-Cr-Mo alloy but lower than the Ti-6Al-4V and cp titanium. It is hoped that diffusion during brazing might dilute the nickel and copper elements and hence improve the corrosion resistance of the three-component brazing alloys investigated.

When recognizing the presence of  $\text{Ti}_2\text{Ni}$  and  $\text{Ti}_2\text{Cu}$  intermetallics in the three-component Ti-15Cu-15Ni and Ti-21Ni-14Cu alloys, a question may be raised as to whether the junction between these alloys and the Ti-6Al-4V could cause galvanic corrosion. To investigate the problem, the  $\text{Ti}_2\text{Ni}$  and  $\text{Ti}_2\text{Cu}$  intermetallics were consolidated and sintered in vacuum by powder metallurgy and the obtained materials were also analyzed for phases and corrosion resistance by the same methods described above. Figure 8 shows the XRD result of the prepared  $\text{Ti}_2\text{Ni}$  and  $\text{Ti}_2\text{Cu}$  materials, in which the  $\text{Ti}_2\text{Cu}$  specimen contains a small amount of  $\text{TiCu}$  phase (JCPDS 7-114). The polarization behavior of  $\text{Ti}_2\text{Ni}$  and  $\text{Ti}_2\text{Cu}$  intermetallics versus

Ti-6Al-4V, shown in Fig. 9, indicates that during a short period of immersion the intermetallics display higher  $E_{\text{corr}}$  potentials and are noble to the Ti-6Al-4V alloy. However, the

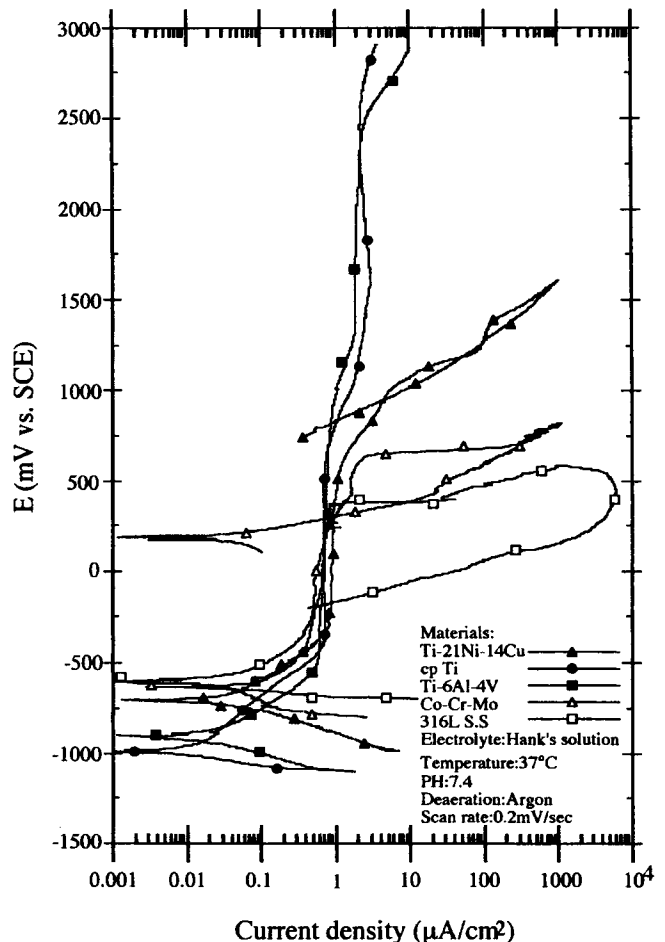


Fig. 7 Comparison of polarization profiles of Ti-21Ni-14Cu alloy, 316L stainless steel, Co-Cr-Mo alloy, Ti-6Al-4V, and cp titanium

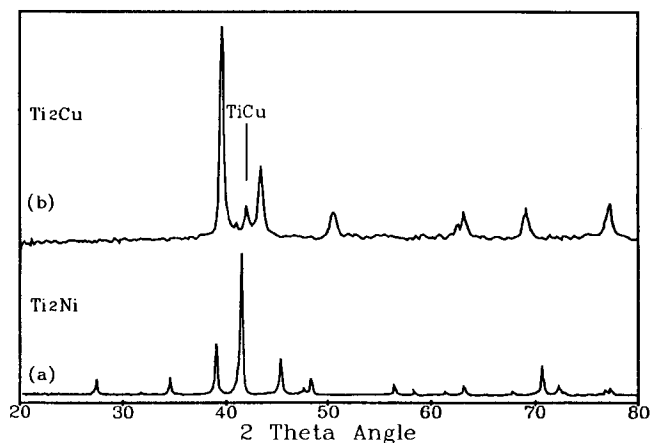


Fig. 8 XRD result of the consolidated (a)  $\text{Ti}_2\text{Ni}$  and (b)  $\text{Ti}_2\text{Cu}$  intermetallics made by powder metallurgy

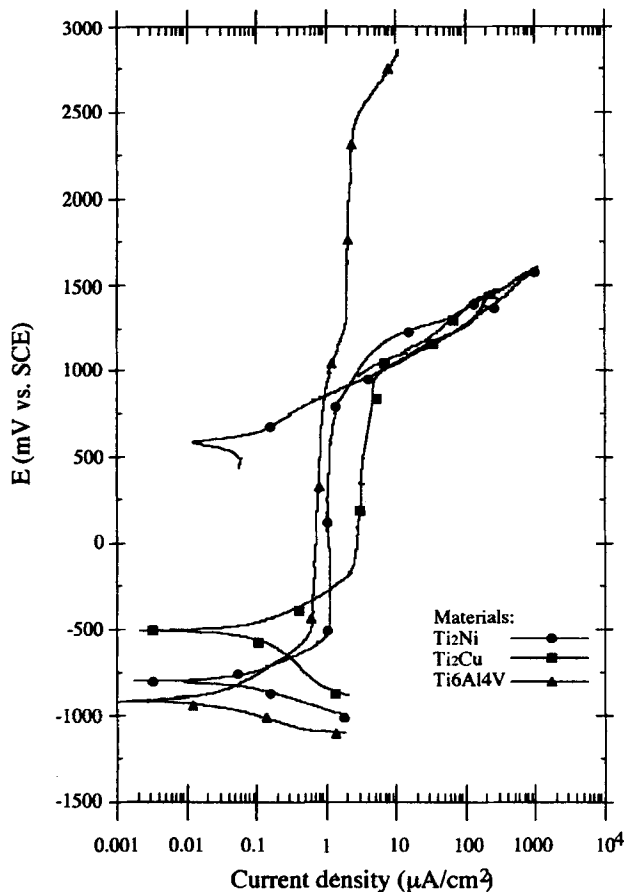


Fig. 9 Potentiodynamic polarization curves of  $Ti_2Ni$  and  $Ti_2Cu$  intermetallics versus  $Ti-6Al-4V$  alloy

result cannot be interpreted that the galvanic corrosion might not occur for the dissimilar alloys of  $Ti_2Ni$  and  $Ti_2Cu$  versus  $Ti-6Al-4V$  because the potentials of titanium alloys are known to vary after immersion in Hank's solution for a period of time (Ref 15).

#### 4. Summary

Five titanium-base filler metals, together with the controls of 316L stainless steel, Co-Cr-Mo alloy,  $Ti-6Al-4V$ , and cp titanium, were studied for their melting point, phase, and electrochemical property. The purpose was to find the potentiality of low-melting-point  $Ti-21Ni-14Cu$  alloy as a brazing filler metal for titanium alloys in terms of the corrosion behavior of the material relative to the various titanium-base filler metals and selected commercial alloys. The polarization test results show that the three-component  $Ti-15Cu-15Ni$  and the newly developed  $Ti-21Ni-14Cu$  alloys possess the attributes of combined lower melting points and superior corrosion resistance to the two- and four-component titanium filler alloys.

In contrast to the 316L stainless steel and Co-Cr-Mo alloy, the  $Ti-21Ni-14Cu$  alloy does not show a distinctively large re-passivation loop; however, this alloy is still considered inferior to  $Ti-6Al-4V$  in its corrosion resistance. However, diffusion during the brazing process might dilute the nickel and copper elements and therefore improve the corrosion resistance of the three-component brazing alloys investigated. On a short time basis, the  $Ti_2Ni$  and  $Ti_2Cu$  intermetallics included in the  $Ti-15Cu-15Ni$  and  $Ti-21Ni-14Cu$  alloys should not be preferentially dissolved as a result of the galvanic corrosion with the  $Ti-6Al-4V$  alloy.

#### References

1. R.Y. Key, L.I. Burnett, and S. Inouye, Titanium Structural Brazing, *Weld. Res. Suppl.*, Vol 53 (No. 10), 1974, p 426-431
2. H.I. McHenry and R.E. Key, Brazed Titanium Fail-Safe Structures, *Weld. Res. Suppl.*, Vol 53 (No. 10), 1974, p 432-439
3. W.T. Kaarlela and W.S. Margolis, Development of the Ag-Al-Mn Brazing Filler Metal for Titanium, *Weld. J.*, Vol. 53 (No. 10), 1974, p 629-636
4. R.R. Well, Low Temperature Large-Area Brazing of Damage Tolerant Titanium Structures, *Weld. Res. Suppl.*, Vol 54 (No. 10), 1975, p 348-356
5. D.G. Howden and R.W. Monroe, Suitable Alloys for Brazing Titanium Heat Exchangers, *Weld. J.*, Vol 51 (No. 1), 1972, p 31-36
6. S.W. Lan, Laminated Brazing Filler Metals for Titanium Assemblies, *Weld. J.*, Vol 61 (No. 10), 1982, p 23-28
7. T. Onzawa, A. Suzumura, and M.W. Ko, Brazing of Titanium Using Low-Melting-Point Ti-Based Filler Metals, *Weld. Res. Suppl.*, Vol. 69 (No. 12), 1990, p 462-467
8. J.C. Chesnutt, C.G. Rhodes, and J.C. Williams, Relationship between Mechanical Properties, Microstructure, and Fracture Topography in  $\alpha + \beta$  Titanium Alloys, *Titanium and Titanium Alloys Source Book*, M.J. Donachie, Jr., Ed., American Society for Metals, 1982, p 100-139
9. S.D. Cook, F.S. Georgette, H.B. Skinner, and R.J. Haddae, Fatigue Properties of Carbon and Porous-Coated  $Ti-6Al-4V$  Alloy, *J. Biomed. Mater. Res.*, Vol 18, 1984, p 497-512
10. M.M. Schwartz, *Brazing*, ASM International, 1985
11. Y.C. Chen, "Studies on New Ti-Cu-Ni Filler Metals for Brazing Titanium Plate," M.S. Thesis, National Sun Yat-Sen University, Taiwan, 1990 (in Chinese)
12. Standard Practice for Standard Reference Method for Making Potentiostatic and Potentiodynamic Anodic Polarization Measurements, G5-82, *Annual Book of ASTM Standards*, Vol 03.02, ASTM, 1983
13. G.I. Ogundele and W.E. White, *Polarization Studies on Surgical-Grade Stainless Steels in Hank's Solution*, STP 859, ASTM, 1985, p 117-135
14. M. Pourbaix, *Atlas of Electrochemical Equilibria in Aqueous Solutions*, Pergamon Press, 1966
15. A.C. Fraker, A.W. Ruff, P. Sung, A.C. Van Orden, and K.M. Speck, Surface Preparation and Corrosion Behavior of Titanium Alloys for Surgical Implants, *Titanium Alloys in Surgical Implants*, STP 796, ASTM, 1983, p 206-219